Journal of Molecular Structure 1020 (2012) 16–22

Contents lists available at SciVerse ScienceDirect

Journal of Molecular Structure

journal homepage: www.elsevier.com/locate/molstruc

Variation in supramolecular arrangements of hydrazones, *o*-$H_2NC_6H_4CMe{=}NNHC_6H_4X$ (X=H, *o*-, *m*- and *p*-NO_2), derived from *o*-aminoacetophenone and phenylhydrazines

R. Alan Howie [a], Thomas C. Baddeley [a], James L. Wardell [b,*], Solange M.S.V. Wardell [c]

[a] Department of Chemistry, University of Aberdeen, Meston Walk, Old Aberdeen AB24 3UE, Scotland, United Kingdom
[b] Centro de Desenvolvimento Tecnológico em Saúde (CDTS), Fundação Oswaldo Cruz, (FIOCRUZ), Casa Amarela, Campus de Manguinhos, Av. Brazil 4365, 21040-900 Rio de Janeiro, RJ, Brazil
[c] CHEMSOL,1 Harcourt Road, Aberdeen AB15 5NY, Scotland, United Kingdom

ARTICLE INFO

Article history:
Received 31 January 2012
Received in revised form 5 April 2012
Accepted 9 April 2012
Available online 20 April 2012

Keywords:
o-Aminophenyl ketones
Hydrazones
Supramolecular arrangements

ABSTRACT

The crystal structures of four hydrazones, **1**, derived from phenylhydrazines, $XC_6H_4NHNH_2$ (X=H, *o*-NO_2, *m*-NO_2 or *p*-NO_2) with 2-aminoacetophenone are reported, as is the mono hydrochloride, (**2**: X=*m*-NO_2), of (**1**: X=*m*-NO_2). Consistent strong intramolecular hydrogen bonds in **1** are of the type, N—$H_{(amino)}\cdots N_{(hydrazono)}$, while (**1**: X=*m*-$NO_2$) portrays an additional N—$H_{(hydrazono)}\cdots O_{(nitro)}$, intramolecular hydrogen bond. Of interest, different sets of strong intermolecular interactions are found even among the nitro derivatives, **1**. In (**1**: X=*o*-NO_2), the strongest intermolecular interactions are N—$H_{(amino)}\cdots O_{(nitro)}$ hydrogen bonds, while in (**1**: X=*m*-NO_2 and *p*-NO_2), both N—$H_{(hydrazono)}\cdots O_{(nitro)}$ and N—$H_{(amino)}\cdots N_{(amino)}$ are present. These strong intermolecular hydrogen bonds coupled with different combinations of some of C—H···O, π—π stacking interactions and N—O···π generate different supramolecular arrays for (**1**: X = nitro): 2-D, 2-D and 3-D, respectively for (**1**: X=*o*-NO_2), for (**1**: X=*m*-NO_2) and (**1**: X=*p*-NO_2). In (**1**: X=H), the major intermolecular interactions are N—$H_{(hydrazono)}\cdots N_{(amino}$ hydrogen bonds: these, supplemented by weaker N—H···π and C—H···π interactions, generate a two-dimensional array.

While significant changes in the intermolecular interactions result on formation of the salt, (**2**: X=*m*-NO_2) from (**1**: X=*m*-NO_2), the strong N—$H_{(amino)}\cdots N_{(hydrazono)}$ intramolecular hydrogen bonds persist. Strong intermolecular hydrogen bonds found in (**2**: X=*m*-NO_2) are of the types N—H···Cl (both hydrazone and amine), N—$H_{(amino)}\cdots O_{(nitro)}$: these coupled with weaker C—H···O, N—O···π, and π—π generate a three dimensional array.

1. Introduction

Our group, over a period of time, has investigated the influence of substituents upon the supramolecular structures in several series of hydrazones. These series include hydrazones formed from substituted phenylhydrazines, including phenylhydrazine itself, and acetone [1], substituted benzaldehydes [2] and 2-hydroxyacetophenone [3]. (Pyrazinecarbonyl)hydrazones of substituted benzaldehydes [4], arylaldehyde 7-chloroquinoline-4-hydrazones [5] and *N*-isonicotinoyl arylaldehyde hydrazones [6] have also been investigated along with *L*-serinyl derivatives, (*S*)-2-hydroxy-1-[*N*-(benzylidene)-hydrazinylcarbonyl]ethylcarbamate esters [7]. We now report the structures of four hydrazones, **1**, generated from $XC_6H_4NHNH_2$ (X=H, *o*-, *m*- or *p*-NO_2) and 2-aminoacetophenone: in addition the structure of the hydrochloride, (**2:** X=*m*-NO_2), of (**1:** X=*m*-NO_2) is also reported, see Fig. 1. Among the aims of this study were an investigation of the changes arising from the positioning of the nitro group substituents in **1** and a comparison of the influence of the *o*-amino and *o*-hydroxyl groups in **1** and *o*-HOC_6H_4NH—N=$CMeC_6H_4X$ (**3**) on the supramolecular arrays generated.

2. Results and discussion

2.1. Synthesis

The syntheses involved reactions of an arylhydrazine or its hydrochloride with an aryl ketone. NMR spectroscopy indicated that in some cases two species, probably the (*E*)- and (*Z*)-isomers, were present in solution, but only the (*E*) isomers were found in the solid state.

* Corresponding author. Tel./fax: +55 2125520435.
E-mail address: j.wardell@abdn.ac.uk (J.L. Wardell).

0022-2860/$ - see front matter © 2012 Elsevier B.V. All rights reserved.
http://dx.doi.org/10.1016/j.molstruc.2012.04.023

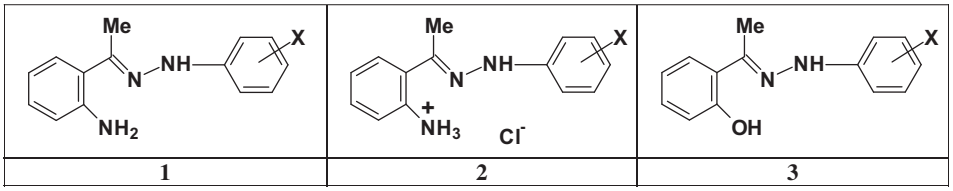

Fig. 1. Compounds whose structures are discussed in this paper.

2.2. Crystal structures

2.2.1. Molecular geometry

The labelling scheme and connectivity of the atoms are shown for **1** and **2** in Fig. 2. The bond lengths and bond angles in **1**–**2** are in the normal ranges for such compounds and are not discussed further except to note that it is the *o*-amino group of (**1**: X=*m*-NO_2) which is protonated on formation of the corresponding hydrochloride, (**2**: X=*m*-NO_2).

Table 1 lists the dihedral angles between the phenyl rings [C(1)—C(6) and C(9)—(14), rings 1 and 2, respectively] with a reference plane (RP), defined by C(7), C(8), N(1), N(2). The largest shifts from overall planarity are exhibited by (**1**: X=*p*-NO_2) and (**2**: X=*m*-NO_2). As indicated by the geometric parameters listed in Table 2, such a result is not a consequence of the differences in the intramolecular hydrogen bonding present in the molecules. Each of the molecules (**1**: X=H, *m*-NO_2 and *p*-NO_2) exhibit solely a strong $N—H_{(amino)}\cdots N_{(hydrazono)}$ intramolecular hydrogen bonds, whereas (**1**: X=*o*-NO_2) portrays an additional strong $N—H_{(hydrazono)}\cdots O_{(nitro)}$

Table 1
Dihedral angles (°) between least squares planes in **1**–**2**. R(1) and R(2) denote the benzene rings in **1**–**2** defined by C(1)—C(6) and C(9)—(14), respectively. The orientation of the benzene rings is relative to a reference plane, RP, defined by C(7)/C(8)/N(1)/N(2), for which the root mean square displacement of the atoms from the least squares plane lies in the range 0.0024–0.0116 Å.

	R(1)/RP	R(2)/RP	R(2)/NO_2
(**1**: X=H)	25.2(2)	20.5(2)	
(**1**: X=*o*-NO_2)	3.99(14)	5.75(14)	1.15(17)
(**1**: X=*m*-NO_2)	6.7(3)	5.0(3)	7.3(5)
(**1**: X=*p*-NO_2)	14.3(3)	9.0(3)	5.8(6)
(**2**: X=*m*-NO_2)	17.40(6)	8.77(7)	4.46(15)

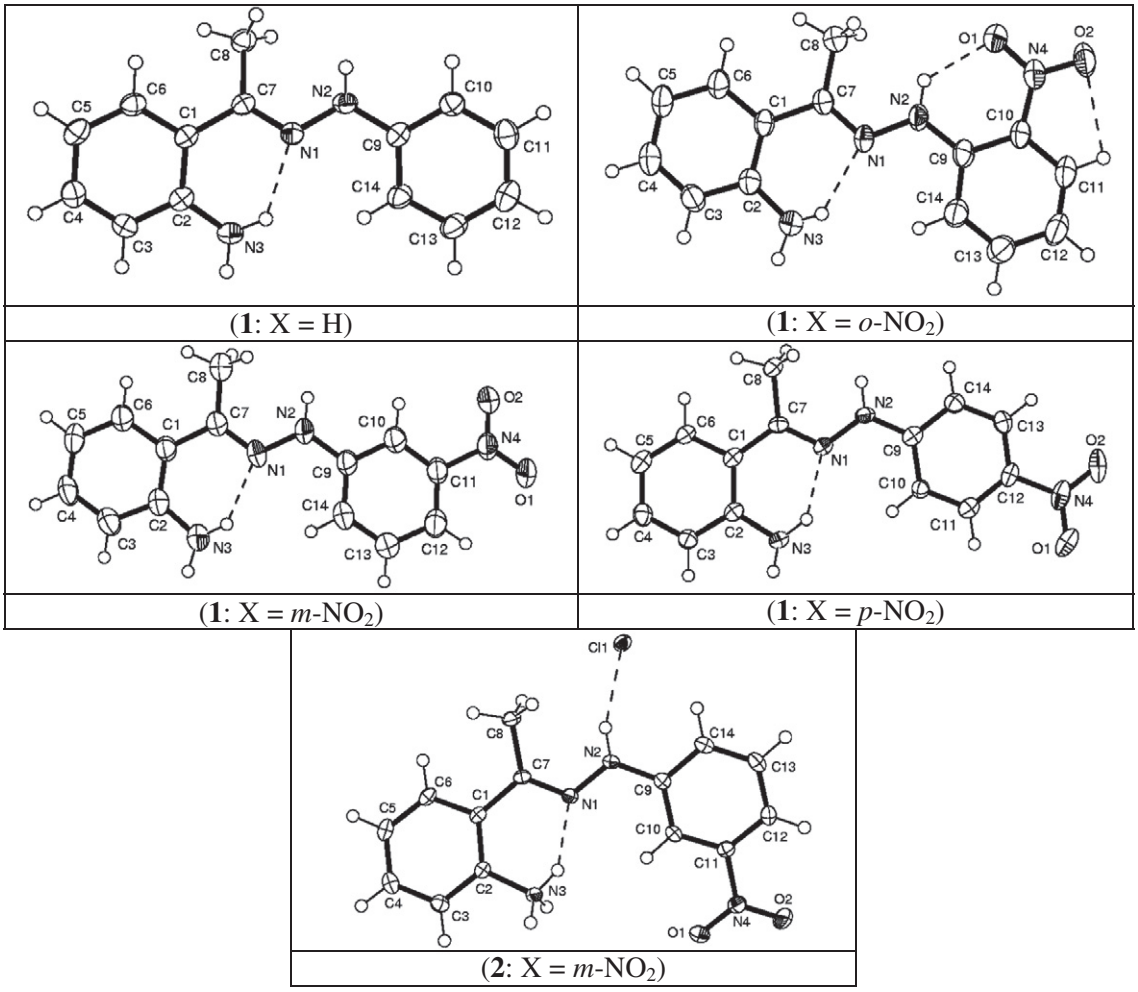

Fig. 2. The labelling and connectivity of the atoms in 1 and 2. Dashed lines represent hydrogen-bonds.

Table 2
Parameters (Å, °) for intramolecular hydrogen-bonds in **1–2**.

Compound	D—H···A	D—H	H···A	D···A	D—H···A
(**1**: X=H)	N(3)—H(3O)···N(1)	0.908(19)	2.04(3)	2.711(4)	130(3)
(**1**: X=*o*-NO_2)	N(2)—H(2 N)···O(1)	0.88	1.95	2.601(7)	129
(**1**: X=*o*-NO_2)	N(3)—H(3O)···N(1)	0.81(7)	2.04(7)	2.643(8)	131(6)
(**1**: X=*o*-NO_2)	C(11)—H(11)···O(2)	0.95	2.36	2.692(8)	100
(**1**: X=*m*-NO_2)	N(3)—H(3O)···N(1)	0.86(4)	2.01(5)	2.675(6)	134(4)
(**1**: X=*p*-NO_2)	N(3)—H(3O)···N(1)	0.95(5)	2.00(5)	2.705(5)	129(3)
(**2**: X=*m*-NO_2)	N(3)—H(3B)···N(1)	0.91	1.99	2.6740(17)	131

as well as a weaker C—H···$O_{(nitro)}$ intramolecular hydrogen bond, see Table 2 and Fig. 2. In the cases of the nitro derivatives of **1**, the nitro group is only slightly out of the plane of the attached phenyl ring, see Table 1. The strong N—$H_{(ammomio)}$···$N_{(hydrazono)}$ intramolecular hydrogen bonds persists on formation of the salt, (**2**: X=*m*-NO_2) from (**1**: X=*m*-NO_2).

2.2.2. Supramolecular connectivity

All of the structures exhibit strong intermolecular (or interionic) hydrogen-bonds of the form X—H···Y, where X=O or N and Y=O, N, Cl and some show weaker interactions, such as C—H···Y (Y=O or π), listed in Table 3. The cut-off values taken for the C—H···O weak hydrogen bonds are d(H···O) < the sum of the van der Waals radii, 2.72 Å, and C—H···O < 100° [8]. The latter interactions while weaker still play important roles in the supramolecular arrays generated [9]. In (**1**: X=H) intermolecular hydrogen-bonds of the form N(2)—H(2N)···N(3) link molecules, related to one another by unit cell translation, to form chains propagated in the direction of **a**, which can be seen at $y = 0$ and 1/2 in Fig. 3a. Links between the chains to complete two-dimensional connectivity in layers of molecules parallel to (0 0 1) are provided by weaker C—H···π interactions of the form N(3)—H(3 N)···Cg(1) and C(5)—H(5)···Cg(2).

The situation in (**1**: X=*o*-NO_2), shown in Fig. 3b, is generally similar except that the connectivity in the chains of molecules related to one another by unit cell translation, now in the direction of **b,** is accomplished by hydrogen-bonds of the form N(3)—H(3 N)···O(1) and connectivity between the chains completing two-dimensional connectivity in layers of molecules, again parallel to (0 0 1), is provided by a combination of π···π interactions (Table 4a) and N—O···π contacts [10] (Table 4b). The cut off values accepted for the N—O···π contacts are d(O···Cg) < 4.0 Å and γ < 30.0° [8].

In (**1**: X=*m*-NO_2) intermolecular hydrogen-bonds of the form N(2)—H(2 N)···O(2) and C(10)—H(10)···O(2) create dimers such as that at the centre of the unit cell as shown in Fig. 4a. The face to face dimers, related to one another by unit cell translation, form stacks, for the choice of origin used in the refinement, propagated along the 1, 0, *z* and 1/2, 1/2, *z* rows. As can be seen in Fig. 4b, where the dimers are seen approximately end on, connectivity within and between the stacks, completing two-dimensional connectivity in layers of molecules parallel to (1 0 1), is provided by hydrogen-bonds of the form N(3)—H(3 N)···N(3') where N(3) of the *o*-NH_2 group is both donor and acceptor.

In (**1**: X=*p*-NO_2), as seen in Fig. 4c, it is the individual molecules, not dimers, which are related to one another by unit cell translation in the direction of **c** to form stacks. There are now two forms of connection both operating between and within the stacks as indicated in Fig. 4d. The first is the same N(3)—H(3 N)···N(3') as before. The second consists of two intermolecular hydrogen-bonds which are of the form N(2)—H(2 N)···O(1) and C(14)—H(14)···O(1) which both utilise the same nitro group oxygen atom as acceptor. Overall, complete three-dimensional connectivity is attained.

As noted above in Section 2.2.1, the hydrochloride, (**2**: X=*m*-NO_2), is formed from (**1**: X=*m*-NO_2) on protonation of the *o*-amino group. The ammonium group acts as a three time donor in intermolecular hydrogen-bonding with two chloride ions and to a nitro oxygen as acceptor, see Table 3. Additionally N(2) in (**2**: X=*m*-NO_2) acts as donor for an intermolecular hydrogen-bond now with another Cl. These four intermolecular hydrogen-bonds together with the weak π···π [Cg(1)···Cg(2), Table 4a] and N—O···π [N(4)—O(2)···Cg(2), Table 4b] contacts create one dimensional connectivity in double chains propagated in the direction of **c** as shown in Fig. 5. The chains are packed side by side in a C-face centred arrangement which induces the C(5)—H(5)···O(1) (Table 3) intermolecular hydrogen-bond and the Cg(1)···Cg(1′) π···π contact (Table 4a) to complete the three-dimensional connectivity of the structure.

In the series of hydrazones, **3**, derived from 2-hydroxyacetophenone and $XC_6H_4NHNH_2$, previously reported [2], the *o*-hydroxy

Table 3
Parameters (Å, °) for intermolecular (or interionic) hydrogen-bonds in **1–2**. Entries of the form X—H···Cg (X=N or C) under the column heading D—H···A indicate X—H···π contacts where Cg(1) and Cg(2) are the centroids of the rings defined by C(1)—C(6) and C(9)—C(14), respectively.

Compound	D—H···A	D—H	H···A	D···A	D—H···A
(**1**: X=H)	N(2)—H(2 N)···$N(3^{i})$	0.89(4)	2.46(4)	3.177(4)	138(3)
(**1**: X=H)	N(3)—H(3 N)···$Cg(1^{ii})$	0.889(19)	2.91(3)	3.651(3)	142(2)
(**1**: X=H)	C(5)—H(5)···$Cg(2^{iii})$	0.95	2.69	3.602(3)	160
(**1**: X=*o*-NO_2)	N(3)—H(3 N)···$O(1^{iv})$	0.90(8)	2.35(7)	3.112(7)	143(6)
(**1**: X=*m*-NO_2)	N(2)—H(2 N)···$O(2^{v})$	0.88	2.30	3.093(6)	150
(**1**: X=*m*-NO_2)	N(3)—H(3 N)···$N(3^{vi})$	0.97(5)	2.19(5)	3.107(7)	157(4)
(**1**: X=*m*-NO_2)	C(10)—H(10)···$O(2^{v})$	0.95	2.44	3.247(7)	143
(**1**: X=*p*-NO_2)	N(2)—H(2 N)···$O(1^{vii})$	0.88	2.52	3.036(5)	118
(**1**: X=*p*-NO_2)	N(3)—H(3 N)···$N(3^{viii})$	0.92(4)	2.32(4)	3.230(5)	168(4)
(**1**: X=*p*-NO_2)	C(14)—H(14)···$O(1^{ix})$	0.95	2.57	3.375(6)	142
(**2**: X=*m*-NO_2)	N(2)—H(2 N)···Cl(1)	0.88	2.59	3.3379(13)	144
(**2**: X=*m*-NO_2)	N(3)—H(3A)···$Cl(1^{x})$	0.91	2.25	3.1375(13)	164
(**2**: X=*m*-NO_2)	N(3)—H(3B)···$O(1^{xi})$	0.91	2.30	2.9519(17)	128
(**2**: X=*m*-NO_2)	N(3)—H(3C)···$Cl(1^{xii})$	0.91	2.22	3.1288(14)	176
(**2**: X=*m*-NO_2)	C(5)—H(5)···$O(1^{xiii})$	0.95	2.49	3.1646(19)	128

Symmetry codes: (i) $x-1, y, z$; (ii) $-x+2, y+1/2, -z+1$; (iii) $-x+1, y-1/2, -z+1$; (iv) $x, y+1, z$; (v) $-x+1, -y+2, -z+1$; (vi) $-x+1/2, y-1/2, -z+3/2$; (vii) $-x+3/2, y-1/2, z-1/2$; (viii) $-x+1, -y+1, z-1/2$; (ix) $-x+3/2, y-1/2, z+1/2$; (x) $x, -y+1, z-1/2$; (xi) $-x+1, y, -z+1/2$; (xii) $-x+1, -y+1, -z+1$; and (xiii) $x+1/2, -y+1/2, z+½$.

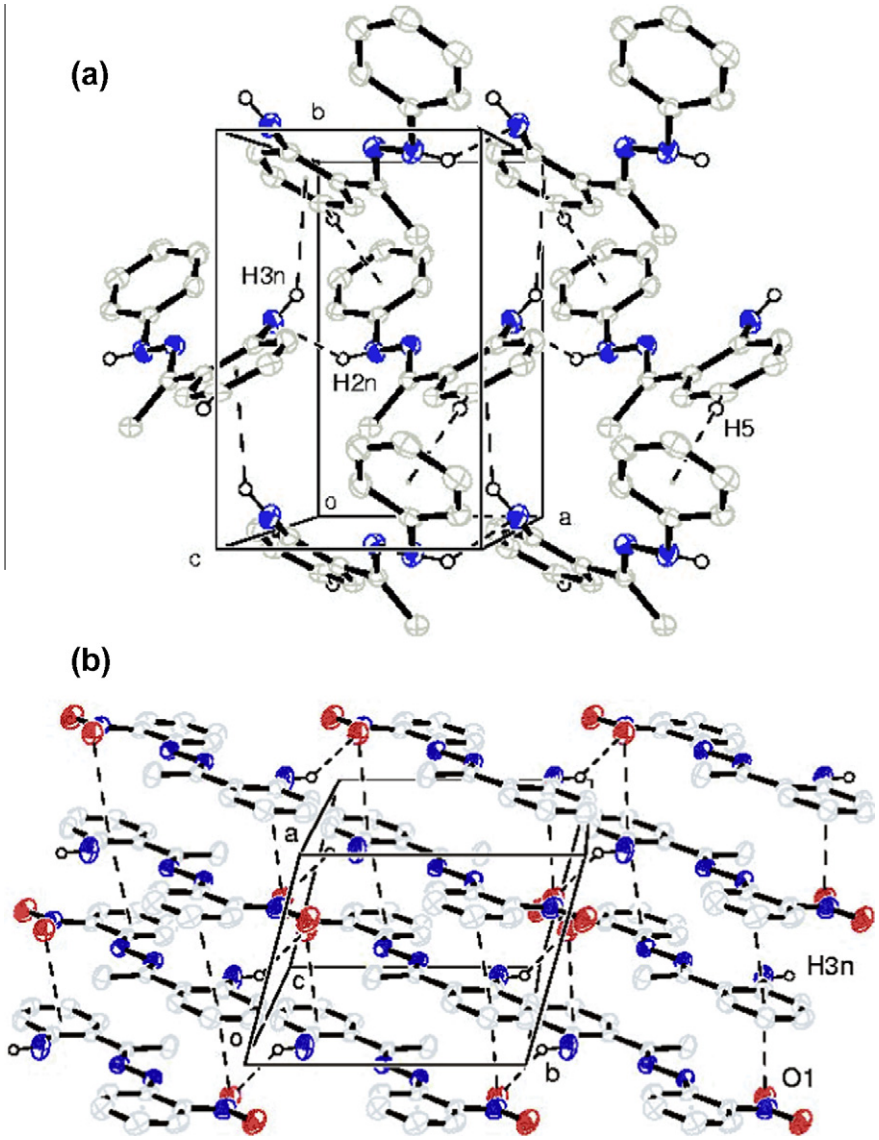

Fig. 3. Intermolecular connectivity (dashed lines) in (a) (1: X=H) and (b) (1: X=*o*-NO_2). The unit cell outlines are shown and selected atoms are labelled.

Table 4
Parameters (Å, °) for further, comparatively weak $\pi\cdots\pi$ and N—O$\cdots\pi$ intermolecular contacts Cg(1) and Cg(2) are the centroids of the rings defined by C(1)—C(6) and C(9)—C(14), respectively.

Compound	Cg(I)···Cg(J)	Cg···Cg	α	β	γ	$Cg(I)_{perp}$	$Cg(J)_{perp}$
a. $\pi\cdots\pi$ intermolecular contacts							
(**1**: X=*o*-NO_2	Cg(1)···Cg(2^{i})	3.720(7)	1.28	23.84	24.76	3.378	3.402
(**2**: X=*m*-NO_2	Cg(1)···Cg(1^{ii})	3.6722(10)	0.0	17.40	17.40	3.504	3.504
(**2**: X=*m*-NO_2	Cg(1)···Cg(2^{i})	3.9019(11)	16.19	31.10	17.53	3.721	3.341
	N—O···Cg	O···Cg	O_{perp}	γ	N—O···Cg	N···Cg	
b. N—O$\cdots\pi$ intermolecular contacts							
(**1**: X=*o*-NO_2	N(4)—O(1)···Cg(1^{i})	3.787(8)	3.475	23.42	68.1(3)	3.517(8)	
(**2**: X=*m*-NO_2	N(4)—O(2)···Cg(2^{ii})	3.6330(19)	3.456	17.94	74.96(11)	3.5199(17)	

Symmetry codes: (i) $-x+1, -y+1, -z+1$; and (ii) $-x+3/2, -y+1/2, -z+1$.
Alpha is the dihedral angle between the least squares planes of the overlapping rings. Beta is the angle between the vectors Cg···Cg and $Cg(I)_{perp}$ where $Cg(I)_{perp}$ is the prependicular distance of Cg(I) from the plane of ring J. Similarly γ is the angle between the vectors Cg···Cg and $Cg(J)_{perp}$.
Symmetry codes: (i) $-x, -y+1, -z+1$; and (ii) $-x+1, y, -z+1/2$.
O_{perp} is the perpendicular distance of the oxygen atom from the ring plane and γ is the angle between the vectors O_{perp} and O···Cg.

group, as does the *o*-amino group in series **1**, is involved in strong hydrogen bonding. Generally, the *o*-hydroxy group acts as a donor in forming intramolecular O—H···N(H) hydrogen bonds, and as an acceptor in forming N—H···O intermolecular hydrogen bonds in (**3**: X=H and 4-NO_2): interestingly, such intermolecular N—H···O hydrogen bonds are absent in (**3**: X=2-NO_2 and 3-NO_2). As with the compounds studied in this article, supramolecular arrangements varied for the individual members of series **3** as a

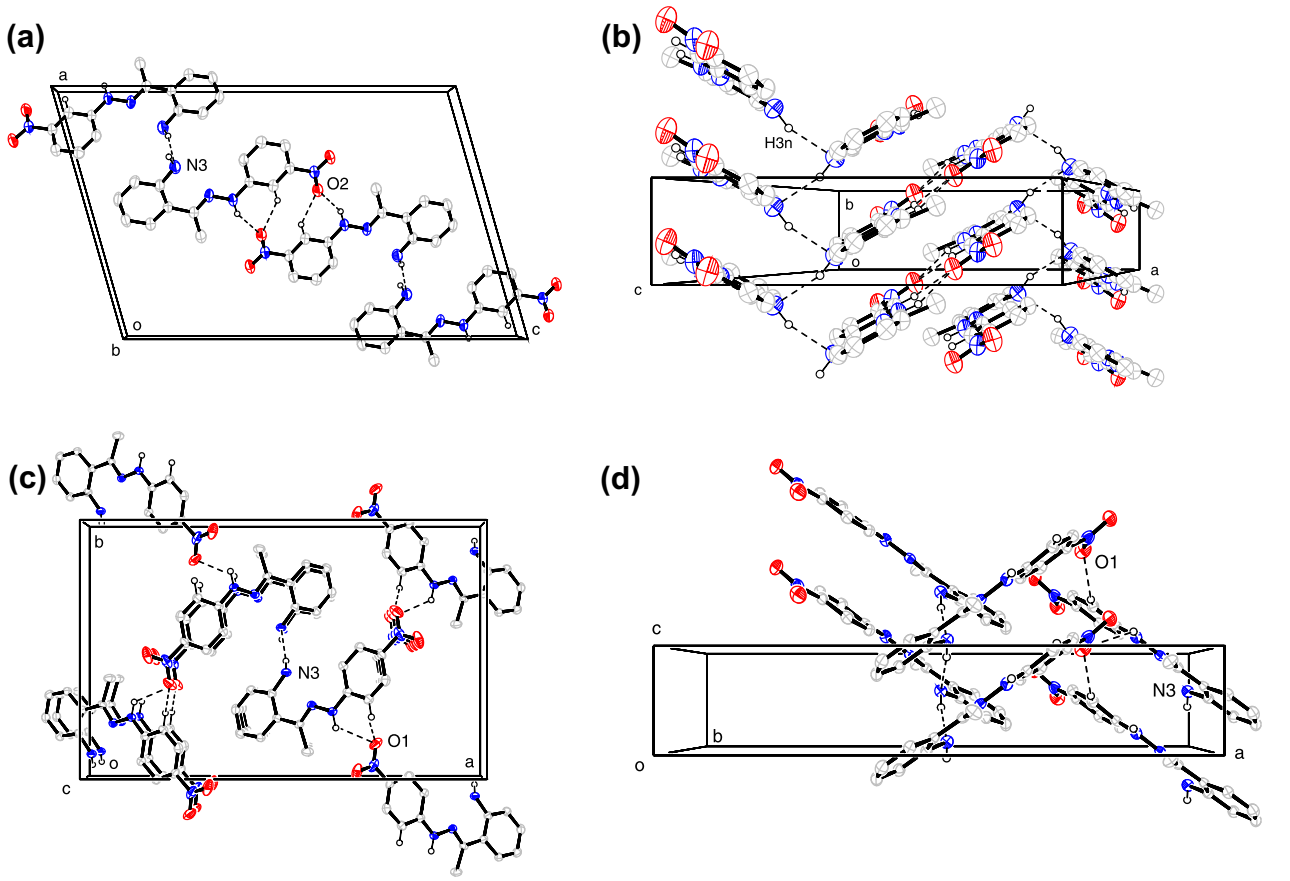

Fig. 4. Intermolecular connectivity (dashed lines) in (a) and (b) (1: X=*m*-NO_2) and (c) and (d) (1: X=*p*-NO_2). The unit cell outlines are shown and selected atoms are labelled.

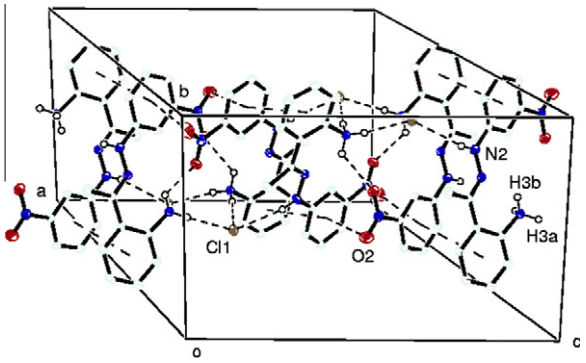

Fig. 5. Double chain in (2: X=*m*-NO_2). Selected atoms are labelled.

consequence of different combinations of intermolecular interactions, which included N—H···O(H), N—H···O(NO), C—H···O(H), C—H···O(NO) and C—H···π hydrogen bonds, as well as $\pi\cdots\pi$ stacking interactions.

3. Experimental

3.1. General

IR spectra were recorded on a Nicolet Magna 760 FTIR instrument. Melting points were measured on a Griffin melting point apparatus. Elemental analyses were performed with a Perkin Elmer 2400 apparatus. Mass spectra were obtained using a Waters Quattro Premier Triple quadruple instrument, in ES + mode, with samples in MeOH solutions, with source T = 100 °C and desolvation T = 150 °C and cone voltage 15 V. Daughter peaks were obtained with a collision voltage of 10 V.

3.2. Synthesis

3.2.1. General procedure

Solutions of an arylhydrazine, or its hydrochloride, and the ketone (1–3 mmol each) in either ethanol or methanol (15–25 ml) were refluxed for 1 h, rotary evaporated and the residue recrystallised from ethanol, methanol or acetone.

3.2.2. (E)-2-Aminoacetophenone phenylhydrazone (*1*: X=H)

Reagents: 2-Aminoacetophenone and phenylhydrazine (2 mmol) in EtOH (20 ml). Recrystallised from EtOH, m.p. 206–8 °C.
IR (KBr, cm^{-1}): v: 3450, 3319, 1615, 1600, 1580.
Anal. Found: C, 74.51; H, 6.92; N, 18.38. Calculated for $C_{14}H_{15}N_3$: C, 74.63; H, 6.71; N, 18.64%.

3.2.3. (E)-2-Aminoacetophenone 2-nitrophenylhydrazone (*1*: X=o-NO_2)

Reagents: 2-Aminoacetophenone and 2-nitrophenylhydrazine (2 mmol) in EtOH (20 ml). Recrystallised from EtOH, m.p. 158–160 °C.
IR (KBr, cm^{-1}): v: 3456, 3318, 1620, 1576.
EI$^+$ MS: 293 [1% (M + Na)$^+$], 271 [100% (M + Na)$^+$], 133 [26% ($C_8H_9N_2$)$^+$, (2-$H_2NC_6H_4CMeN$)].

Table 5
Crystal data and structure refinement for 1 and 2.

	(**1**: X=H)	(**1**: X=*o*-NO_2)	(**1**: X=*m*-NO_2)	(**1**: X=*p*-NO_2)	(**2**: X=*m*-NO_2)
Empirical formula	$C_{14}H_{15}N_3$	$C_{14}H_{14}N_4O_2$	$C_{14}H_{14}N_4O_2$	$C_{14}H_{14}N_4O_2$	$C_{14}H_{15}ClN_4O_2$
Formula weight	225.29	270.29	270.29	270.29	306.75
Crystal system, space group	Monoclinic, $P2_1$	Triclinic, *P*-1	Monoclinic, $P2_1/n$	Orthorhombic, $Pna2_1$	Monoclinic, $C2/c$
Unit cell dimensions:					
a (Å)	5.9544(3)	6.8201(10)	14.91(2)	21.666(1)	18.3030(4)
b (Å)	9.4214(5)	8.633(13)	3.898(6)	13.8168(6)	10.4042(3)
c (Å)	10.8369(6)	11.326(18)	22.89(4)	4.1612(1)	16.4597(3)
α (°)	90	81.76(3)	90	90	90
β (°)	99.746(3)	88.29(4)	105.906(15)	90	114.998 (1)
γ (°)	90	75.99(4)	90	90	90
Volume (Å^3)	599.16(6)	640.3(14)	1279(3)	1245.68(8)	2840.77(12)
Z, Calculated density (Mg/m^3)	2, 1.249	2, 1.402	4, 1.403	4, 1.441	8, 1.434
Absorpt. coefficient (mm^{-1})	0.076	0.098	0.098	0.101	0.279
F(000)	240	284	568	568	1280
Crystal size (mm)	0.10 × 0.08 × 0.04	0.05 × 0.04 × 0.01	0.08 × 0.03 × 0.005	0.38 × 0.02 × 0.02	0.36 × 0.34 × 0.15
Theta range for data collection (°)	3.47–27.69	2.38–26.82	1.79–22.50	2.95–27.52	3.16–27.50
Index ranges	$-7 \leqslant h \leqslant 7$ $-12 \leqslant k \leqslant 12$ $-14 \leqslant l \leqslant 14$	$-8 \leqslant h \leqslant 6$ $-11 \leqslant k \leqslant 11$ $-14 \leqslant l \leqslant 14$	$-16 \leqslant h \leqslant 16$ $-3 \leqslant k \leqslant 4$ $-25 \leqslant l \leqslant 25$	$-28 \leqslant h \leqslant 27$ $-9 \leqslant k \leqslant 17$ $-5 \leqslant l \leqslant 4$	$-23 \leqslant h \leqslant 23$ $-13 \leqslant k \leqslant 12$ $-21 \leqslant l \leqslant 21$
Reflections collected/unique	7822/1469 [***R***(int) = 0.088]	6300/2815 [***R***(int) = 0.039]	7669/1840 [***R***(int) = 0.103]	7130/1617 [***R***(int) = 0.066]	17.579/3257 [***R***(int) = 0.046]
Reflections observed [$I > 2\sigma(I)$]	1070	1467	925	1289	2685
Max. and min. transmission	0.9969 and 0.8680	0.9990 and 0.6893	0.9995 and 0.9922	0.9980 and 0.8312	0.9593 and 0.8800
Data/restraints/parameters	1469/3/165	2815/0/190	1840/0/188	1617/1/188	3257/0/192
Goodness-of-fit on F^2	1.049	1.107	0.972	1.177	1.060
Final *R* indices [$I > 2\sigma(I)$]	$\boldsymbol{R_1}$ = 0.055, $\boldsymbol{wR_2}$ = 0.113	$\boldsymbol{R_1}$ = 0.107, $\boldsymbol{wR_2}$ = 0.350	$\boldsymbol{R_1}$ = 0.061, $\boldsymbol{wR_2}$ = 0.157	$\boldsymbol{R_1}$ = 0.065, $\boldsymbol{wR_2}$ = 0.117	$\boldsymbol{R_1}$ = 0.038, $\boldsymbol{wR_2}$ = 0.093
R indices (all data)	$\boldsymbol{R_1}$ = 0.090, $\boldsymbol{wR_2}$ = 0.129	$\boldsymbol{R_1}$ = 0.155, $\boldsymbol{wR_2}$ = 0.373	$\boldsymbol{R_1}$ = 0. 129, $\boldsymbol{wR_2}$ = 0.197	$\boldsymbol{R_1}$ = 0.091, $\boldsymbol{wR_2}$ = 0.130	$\boldsymbol{R_1}$ = 0.049, $\boldsymbol{wR_2}$ = 0.099
Largest diff. peak and hole (e/Å^3)	0.20 and −0.21	0.40 and −0.43	0.23 and −0.24	0.27 and −0.24	0.27 and −0.27

MSMS on m/z = 271: m/z = 271 [19% $(M + H)^+$], 133 [100%, $(C_8H_9N_2)^+$].
Anal. Found: C, 62.45; H, 5.01; N, 20.54. Calculated for $C_{14}H_{14}N_4O_2$: C, 62.21; H, 5.22; N, 20.72%.

3.2.4. (E)-2-Aminoacetophenone 3-nitrophenylhydrazone (*1: X=m-NO$_2$)*

Reagents: 2-Aminoacetophenone and 3-nitrophenylhydrazine (2 mmol) in EtOH (25 ml). Recrystallised from EtOH, m.p. 178–181 °C.
IR (KBr, cm^{-1}): v: 3460, 3339, 1620, 1605, 1587.
EI$^+$ MS: m/z = 563 [4% $(2\ M + Na)^+$], 541 [17% $(2\ M + H)^+$, 293 [3% $(M + Na)^+$], 271 [100% $(M + Na)^+$].
MSMS on m/z = 271: m/z = 271 [100% $(M + H)^+$], 254 [12% $(M - 16)^+$], 208 [22% $(M - 62)^+$], 134 [47%, $(C_8H_{10}N_2)^+$], 133 [8%, $(C_8H_9N_2)^+$], 120 [31%], 106 [4%].
Anal. Found: C, 62.39; H, 5.32; N, 20.48. Calculated for $C_{14}H_{14}N_4O_2$: C, 62.21; H, 5.22; N, 20.72%.

3.2.5. (E)-2-Aminoacetophenone 4-nitrophenylhydrazone (*1: X=p-NO$_2$)*

Reagents: 2-Aminoacetophenone and 4-nitrophenylhydrazine (2 mmol) in EtOH (25 ml). Recrystallised from EtOH, m.p. 195–6 °C.
IR (KBr, cm^{-1}): v: 3375, 3328, 1597(br).
EI$^+$ MS: m/z = 563 [2% $(2\ M + Na)^+$], 541 [2% $(2\ M + H)^+$], 293 [1% $(M + Na)^+$], 271 [100% $(M + Na)^+$], 133 [7%, $(C_8H_9N_2)^+$].
MSMS on m/z = 271: m/z = 271 [100% $(M + H)^+$], 254 [9% $(M - 16)^+$], 208 [5% $(M - 62)^+$], 206 [16% $(M - 62)^+$134 [60%, $(C_8H_{10}N_2)^+$], 133 [14%, $(C_8H_9N_2)^+$], 120 [41%], 106 [3%].
Anal. Found: C, 62.35; H, 5.17; N, 20.57. Calculated for $C_{14}H_{14}N_4O_2$: C, 62.21; H, 5.22; N, 20.72%.

3.2.6. (E)-2-Aminoacetophenone 3-nitrophenylhydrazone hydrochloride (*2: X=m-NO$_2$)*

Reagents: 2-Aminoacetophenone and 3-nitrophenylhydrazine.hydrochloride (2 mmol) in EtOH (20 ml). Recrystallised from Me_2CO.
IR (KBr, cm^{-1}): v: 3300–2300(v.br), 3258, 1618, 1580, 1535, 1515.
Anal. Found: C, 54.97; H, 5.14; N, 18.02. Calculated for $C_{14}H_{15}ClN_4O_2$: C, 54.81; H, 4.94; N, 18.26%.

3.3. Crystallography

In all cases the intensity data were collected at 120(2) K. For (**1**: X=*o*-NO_2) and (**1**: X=*m*-NO_2) the data were obtained with synchrotron radiation [11] (λ = 0.6889 Å) at beamline I19 of the EPSRC Diamond Light Source at the Harwell Science and Innovation Campus, Didcot, UK, by staff of the National X-ray crystallographic service utilising a Rigaku Saturn 724 + detector on a Crystal Logics diffractometer. Data collection, cell refinement and data reduction were accomplished with the CrystalClear [12] software package. For (**1**: X=*o*-NO_2) only, correction for absorption, by comparison of the intensities of equivalent reflections, was applied by means of the programme, SADABS [13].

For all other cases the data were obtained with Mo Kα radiation (λ = 0.71073 Å) on a Bruker-Nonius KappaCCD area detector diffractometer of the EPSRC X-ray crystallographic service at the University of Southampton, UK. Data collection was carried out under the control of the program COLLECT [14] and data reduction and unit cell refinement were achieved with the COLLECT and DENZO [15] software combination. Correction for absorption was applied by means of the program SADABS [16]. The structures were solved by direct methods in SHELXS97 [17] and refined, by full-matrix least-squares on $\boldsymbol{F^2}$, in SHELXL97 [17], both within the OSCAIL [18] suite of programs.

Coordinates of the hydrogen atoms of all of the NH_2 groups in **1**, the NH group in (**1**: X=H) were obtained from difference maps and refined freely. All other hydrogen atoms were placed in calculated positions with X—H distances (X=O, N or C) of Å 0.84, 0.88, 0.91, 0.95 or 0.98 Å for OH, NH or NH_3 groups or aryl or methyl hydrogen, respectively, and refined with a riding model. For all hydrogen atoms $U_{iso}(H)$ was set to $kU_{eq}(X)$ with $k = 1.5$ for NH_3 and methyl groups and H_2O and 1.2 otherwise. The rotational orientations of the methyl and NH_3 groups were also refined. The refinements of (**1**: X=H) and (**1**: X=*p*-NO_2) were carried out, as is the normal practice for non-centrosymmetric structures containing no atom of higher atomic number than that of oxygen, with merged intensity data so that the absolute structures are indeterminate and the Flack x parameters [19] meaningless and therefore not reported. In the case of (**1**: X=H) correction for extinction was applied where the coefficient k in the correction of the form $\boldsymbol{F}c^* = k\boldsymbol{F}c[1 + 0.001 \times \boldsymbol{F}c^2\lambda^3/\sin(2\theta)]^{-1/4}$ was refined to the value of 0.047(12). The program ORTEP-3 for Windows [20] has been used in the preparation of the Figures in which ellipsoids are drawn at the 50% probability level and hydrogen atoms, where shown, are represented as small spheres of arbitrary radii. Where colour coding is used C, Cl, N and O are shown as open, green, blue and red ellipsoids, respectively. Programs SHELXL97 [17] and PLATON [8] were used in the calculation of molecular geometry. Hydrogen bonds of the form C—H···X (X=Cl or O) were identified by PLATON but their geometric parameters were calculated by SHELXL97. Crystal data and structure refinement details are listed in Table 5 for **1** and **2**.

4. Conclusions

Consistant strong intramolecular hydrogen bonds present in **1** are of the type, $N—H_{(amine)}\cdots N_{(hydrazone)}$, while (**1**: X=*o*-$NO_2$) portrays an additional $N—H_{(hydrazone)}\cdots O_{(nitro)}$ intramolecular hydrogen bond. Different sets of strong intermolecular interactions are found even among the nitro derivatives, **1**. In (**1**: X=*o*-NO_2), the strongest intermolecular interactions are $N—H_{(amine)}\cdots O_{(nitro)}$ hydrogen bonds, while in (**1**: X=*m*-NO_2 and *p*-NO_2), both $N—H_{(hydrazone)}\cdots O_{(nitro)}$ and $N—H_{(amine)}\cdots N_{(amino)}$ are present. These strong intermolecular hydrogen bonds coupled with different combinations of some of C—H···O, $\pi\cdots\pi$ stacking interactions and N—O—π generate different supramolecular arrays. In (**1**: X=H), the major intermolecular interactions are $N—H_{(hydrazone)}\cdots N_{(amine)}$ hydrogen bonds. While significant changes in the intermolecular interactions result on formation of the salt, (**2**: X=*m*-NO_2) from (**1**: X=*m*-NO_2), the strong $N—H_{(ammonio)}\cdots N_{(hydrazone)}$ intramolecular hydrogen bonds persist. Strong intermolecular hydrogen bonds found in (**2**: X=*m*-NO_2) are of the types N—H···Cl (both hydrazone and amine), $N—H_{(amine)}\cdots$O(nitro).

In the series of hydrazones, **3**, derived from 2-hydroxyacetophenone and $XC_6H_4NHNH_2$, previously reported [2], the hydroxy groups formed strong intramolecular O—H···N(H) hydrogen bonds for all compounds. As with the compounds studied in this article, supramolecular arrangements varied for the individual members of series **3** as a consequence of different combinations of intermolecular interactions, which included C—H···O(H) and C—H···O(NO), N—H···O(H), N—H···O(NO) and C—H···π hydrogen bonds, as well as $\pi\cdots\pi$ stacking interactions.

Acknowledgements

The use of the EPSRC X-ray crystallographic service at Southampton and the valuable assistance of the staff there is gratefully acknowledged. We thank CAPES for financial support.

Appendix A. Supplementary data

Full details of the crystal structure determinations in cif format are available in the online version, at doi: (to be inserted), and have also been deposited with the Cambridge Crystallographic Data Centre with deposition numbers 852597–852600 and 852602 for refinements of (**1**: X=H), (**1**: X=*o*-NO_2), (**1**: X=*m*-NO_2), (**1**: X=*p*-NO_2) and (**2**: X=*m*-NO_2) respectively. Copies of these can be obtained free of charge on written application to CCDC, 12 Union Road, Cambridge, CB2 1EZ, UK (fax: +44 1223 336033); on request by e-mail to deposit@ccdc.cam.ac.uk or by access to http://www.ccdc.cam.ac.uk. Supplementary data associated with this article can be found, in the online version, at http://dx.doi.org/10.1016/j.molstruc.2012.04.023.

References

[1] S.M.S.V. Wardell, M.V.N. de Souza, J.L. Wardell, J.N. Low, C. Glidewell, C.: Acta Crystallogr. E 62 (2006) o2838–o2840.;
J.L. Wardell, J.N. Low, C. Glidewell, C. Acta Crystallogr, C 63 (2007) o231–o233.
[2] G. Ferguson, C. Glidewell, J.N. Low, J.M.S. Skakle, J.L. Wardell, Acta Crystallogr. C61 (2005) o613–o616;
J.L. Wardell, J.M.S. Skakle, J.N. Low, C. Glidewell, Acta Crystallogr. C 61 (2005) o10–o14.
[3] T.C. Baddeley, L. de Souza França, R.A. Howie, G.M. de Lima, J.M.S. Skakle, J.D. de Souza, J.L. Wardell, S.M.S.V. Wardell, Z. Kristallogr. 224 (2009) 213–224.
[4] R.A. Howie, C.H. da Silva Lima, C.R. Kaiser, M.V.N. de Souza, J.L. Wardell, S.M.S.V. Wardell, Z. Kristallogr. 225 (2010) 349–358 and references therein.
[5] R.A. Howie, M.V.N. de Souza, M. de Lima Ferreira, C.R. Kaiser, J.L. Wardell, S.M.S.V. Wardell, Z. Kristallogr. 225 (2010) 440–447.
[6] S.M.S.V. Wardell, M.V.N. de Souza, J.L. Wardell, J.N. Low, C. Glidewell, Acta Crystallogr. B 63 (2007) 879–895 (e.g.).
[7] R.A. Howie, M.V.N. de Souza, A.C. Pinheiro, C.R. Kaiser, J.L. Wardell, S.M.S.V. Wardell, Z. Kristallogr. 226 (2011) 483–491.
[8] A.L. Spek, J. Appl. Crystallogr. 36 (2003) 7–13.
[9] K. Merz, V. Vasylyeva, CrystEngComm. 12 (2010) 3989-4002; D.M.P. Mingos (Ed.), Supramolecular Assembly via Hydrogen Bonds I and II (Structure and Bonding, vols. 108 and 111), Springer, Berlin/Heidelberg, 2004; G.R. Desiraju, T. Steiner, The Weak Hydrogen Bond, Oxford University Press, New York, 1999; M. Nishio, CrystEngComm.6 (2004) 130–158.
[10] L. Huang, L. Massa, J. Karle, Proc. Natl. Acad. Sci. 105 (2008) 13720–13723.
[11] W. Clegg, J. Chem. Soc., Dalton Trans. (2000) 3223–3232.
[12] CrystalClear, Rigaku Inc., The Woodlands, Texas, USA, 2010.
[13] SADABS, Bruker AXS Inc., Madison, USA, 2008.
[14] R.W.W. Hooft, COLLECT, Data Collection Software. Nonius BV, Delft, The Netherlands, 1998.
[15] Z. Otwinowski, W. Minor, Processing of X-ray diffraction data collected in oscillation mode, in: C.W. Carter Jr, R.M. Sweet (Eds.), Methods in Enzymology, Macromolecular Crystallography, Part A, vol. 276, Academic Press, New York, 1997, pp. 307–326.
[16] G.M. Sheldrick, SADABS Version 2007/2, Bruker AXS Inc., Madison, Wisconsin, USA, 2007.
[17] G.M. Sheldrick, Acta Crystallogr. A 64 (2008) 112–122.
[18] P. McArdle, P. OSCAIL for Windows, Version 1.0.12, Crystallography Centre, Chemistry Department, NUI Galway, Ireland, 2006.
[19] H.D. Flack, Acta Crystallogr. A 39 (1983) 876–881.
[20] L. Farrugia, J. Appl. Crystallogr. 30 (1997) 565.